International Journal of Mass Spectrometry 305 (2011) 151–156

Contents lists available at ScienceDirect

International Journal of Mass Spectrometry

journal homepage: www.elsevier.com/locate/ijms

Mass spectrometric analysis of mycothiol levels in wild-type and mycothiol disulfide reductase mutant *Mycobacterium smegmatis*

Cynthia M. Holsclaw[a], Wilson B. Muse III[b], Kate S. Carroll[b], Julie A. Leary[a,*]

[a] *Department of Molecular and Cell Biology, University of California, One Shields Avenue, Davis, CA 95616, USA*
[b] *Life Sciences Institute, 210 Washtenaw Avenue, University of Michigan, Ann Arbor, MI 48109, USA*

ARTICLE INFO

Article history:
Received 23 June 2010
Received in revised form 16 October 2010
Accepted 20 October 2010
Available online 30 October 2010

Keywords:
Tuberculosis
Mycobacteria
Mycothiol
Carbohydrate
Redox balance
Ion trap
Selected ion monitoring

ABSTRACT

Mycothiol (MSH), the primary low-molecular weight thiol produced in mycobacteria, acts to protect the cell from oxidative stress and to maintain redox homeostasis, notably in the pathogenic *Mycobacterium tuberculosis* in the course of human infection. The mycothiol disulfide reductase (Mtr) enzyme reduces the oxidized form of mycothiol, mycothione (MSSM), back to MSH, however its role in bacterial viability is not clear. In this study, we sought to determine the MSH levels of wild-type (WT) and Mtr mutant mycobacteria during oxidative stress. We describe a rapid method for the relative quantification of MSH using high-sensitivity mass spectrometry (MS) with selected ion monitoring (SIM). This method uses only minimal sample cleanup, and does not require advanced chromatographic equipment or fluorescent compounds. MSH levels decreased in the Mtr mutant only upon treatment with peroxide, and the results were consistent between our method and previously described thiol quantification methods. Our results indicate that our MS-based method is a useful, high-throughput alternative tool for the quantification of MSH from mycobacteria.

1. Introduction

Tuberculosis (TB) affects approximately one third of the world's population and kills approximately two million people a year [1]. The causative agent of TB, *Mycobacterium tuberculosis*, is introduced into the human host through inhalation of aerosolized bacteria [2,3]. Once inside the lungs, *M. tuberculosis* is phagocytosed by alveolar macrophages, where it is able to bypass the normal phagosome maturation process and escape into the cytosol of the cell [4–6]. The infected macrophage produces pro-inflammatory signals that recruit T-cells and neutrophils, which wall off the *M. tuberculosis* infection inside a structure called a granuloma [7]. The environment of the granuloma is hypoxic, low in pH, and high in reactive oxygen species (ROS) and reactive nitrogen intermediates (RNI) [7]. In spite of this adverse environment, the bacteria are able to survive inside the granuloma in a latent state for many decades.

M. tuberculosis produces a number of compounds to counteract the ROS and RNI assault by the human immune system. Among these compounds are catalase, peroxidases, and nitrosothiol reductase [8–10], however mycobacteria also produce a low molecular-weight thiol termed mycothiol (MSH) [11]. Mycothiol, an unusual conjugate of *N*-acetylcysteine and 1D-myo-inosityl 2-acetamido-2-deoxy-D-glucopyranoside [11], is the functional equivalent of glutathione in mycobacteria, and is thought to play a key role in the mitigation of oxidative stress on the bacterium. Mycothiol is present in mycobacteria at millimolar levels [11], and is synthesized in a five-step pathway from glucose-6-phosphate through the actions of the Ino1, MshA, MshB, MshC, and MshD enzymes [12–15]. While MSH is thought to be essential to the survival of the bacterium, a recent study demonstrated that *M. tuberculosis* bacteria containing mutations in the *mshA* gene do not produce detectable levels of MSH [16]. Interestingly, these mutants are viable *in vitro* and in the mouse model of *M. tuberculosis* infection [16], suggesting that the role of MSH during infection is much less clear than originally thought.

While recent studies suggest that *M. tuberculosis* uses MSH in detoxification reactions [17,18], its primary function is to relieve the cell from the negative effects of oxidative stress and maintain redox balance. When subjected to oxidative stress, MSH is oxidized to mycothione (MSSM), a dimer of two MSH molecules linked through a disulfide bond. To maintain high levels of MSH in the cell, mycothiol disulfide reductase, or Mtr, cleaves the disulfide bond of MSSM using reducing power from NADPH [19]. It is not entirely clear if Mtr is essential to the viability of the bacterium; a Himar-1

Abbreviations: MSH, mycothiol; Mtr, mycothiol disulfide reductase; MSSM, mycothione; WT, wild-type; SIM, selected ion monitoring; ROS, reactive oxygen species; RNI, reactive nitrogen intermediates; TIC, total ion count; IS, internal standard; mBBr, monobromobimane.

* Corresponding author. Tel.: +1 530 752 4685; fax: +1 530 752 3085.
E-mail address: jaleary@ucdavis.edu (J.A. Leary).

1387-3806/$ – see front matter © 2010 Elsevier B.V. All rights reserved.
doi:10.1016/j.ijms.2010.10.027

transposon mutagenesis screen indicated that *mtr* is essential to *M. tuberculosis* viability [20], while a Tn5370 transposon mutant in *mtr* was reported as viable [21]. If Mtr is not required for the reduction of MSSM, it is possible that a surrogate protein reductant is acting in its place. Conversely, it is possible that MSH is produced at such a high level that the bacterium can overcome the lack of a reducing enzyme [22].

In order to further investigate the role of Mtr in the mitigation of oxidative stress on the bacterium, we sought to determine the relative levels of MSH between WT and *mtr* mutant mycobacteria. For our experiments, we chose the fast growing, nonpathogenic *Mycobacterium smegmatis* as a model organism of mycobacterial biology. While we also employed the previously described bimane-conjugation method of MSH quantification [23], we sought to develop a rapid, mass spectrometry-based method of MSH detection. In this study, we describe a rapid method for the relative quantification of MSH levels from *M. smegmatis*, utilizing high-sensitivity electrospray ionization mass spectrometry (ESI-MS).

2. Materials and methods

2.1. Chemicals and materials

Chloroform, methanol, acetonitrile, glycerol, formic acid, and N,N-diacetylchitobiose were purchased from Fisher Scientific (Pittsburg, PA). The chloroform, methanol and acetonitrile were of HPLC grade. Oasis™ HLB extraction cartridges, 1 cm^3, were obtained from Waters Corporation (Milford, MA). Middlebrook 7H9 and ADC supplement were purchased from Difco Laboratories (Detroit, MI), hydrogen peroxide was obtained from Sigma (St. Louis, MO), and monobromobimane (mBBr) was obtained from Molecular Probes (Carlsbad, CA).

2.2. Bacterial strains and culture conditions

M. smegmatis mc^2155 WT and *mtr* were grown in Middlebrook 7H9 broth supplemented with 10% ADC. Cultures were grown at 30 °C in 10 ml of medium in 75 ml Erlenmeyer culture flasks with gentle shaking at 200 rpm. The detailed construction of the *mtr* mutant will be described and reported elsewhere. Briefly, the *mtr* mutant was constructed by the standard method of allelic replacement. A 1 kb section in the middle of the *mtr* gene was excised and replaced by a *kanR* gene to disrupt the expression and function of the *mtr* gene product, without disrupting any regulatory elements in the surrounding region.

2.3. Determination of mycothiol levels by HPLC

Derivatization of cell extracts with mBBr to determine the thiol content was performed essentially as described [24]. In brief, cell pellets were suspended in 50% aqueous acetonitrile, 2 mM mBBr, and 20 mM HEPES (pH 8). The suspensions were then incubated in the dark at 60 °C for 15 min. After the incubation period, cell debris was removed by centrifugation and the supernatant was diluted four-fold in 10 mM HCl. Control samples were extracted with 50% aqueous acetonitrile, 5 mM *N*-ethylmaleimide, 20 mM HEPES (pH 8.0). The suspensions were incubated again for 15 min at 60 °C. After addition of 2 mM mBBr, the suspensions were incubated again for 15 min at 60 °C and processed as described above. Samples were analyzed by reversed-phase high-performance liquid chromatography (Ultrasphere ODS, C-18 Analytical, 4.6 mm ID × 250 mm) and the eluate was monitored by fluorescence detection (375 nm excitation and 475 nm emission). The column was eluted with 0.25% acetic acid pH 3.6 (buffer A) and 95% methanol (buffer B) at a flow rate of 1 ml/min with the following gradient: initial conditions, 10% buffer B; at 15 min, 18% buffer B; at 30 min, 27% buffer B; at 33 min, 100% buffer B followed by re-equilibration in 10% buffer B.

2.4. Sample preparation for MS analysis

The samples were re-suspended in 5 ml 250 mM formic acid, and a 1-ml aliquot of each sample was run through 1 cm^3 Oasis™ HLB extraction cartridges previously conditioned with methanol and equilibrated with water, to separate the carbohydrates from the lipids in these extracts. After the samples were loaded onto the cartridge, 1 ml of water was added to elute the remaining carbohydrates. The flowthrough was saved, and triplicate aliquots of 200 μl per sample were evaporated to dryness. The samples were resuspended in 50 μl 1:1 acetonitrile:water containing 10 μM of the N,N-diacetylchitobiose internal standard (IS) prior to MS analysis.

2.5. ESI linear ion trap MS

Mass spectra for relative quantification were obtained on an LTQ ion trap mass spectrometer equipped with an electrospray ionization source (Thermo Electron, San Jose, CA). Ions were introduced into the ion source via direct injection at a rate of 5 μl/min, or loop injection at a rate of 10 μl/min. Spectra were obtained in the negative ion mode, using a spray voltage of 3.5 kV and a capillary temperature of 225 °C. Selected ion monitoring (SIM) mode was used for quantification, focusing on the total ion count (TIC) peak areas representing the IS and MSH ions. Spectra are an average of 40 scans, and were acquired using Xcalibur, version 1.4 (ThermoFinnigan). Forty scans for each of the IS and MSH peaks were averaged to determine their peak intensity ratio (I_{MSH}/I_{IS}). Each sample was analyzed three times (three separate injections) to produce triplicate technical replicates.

2.6. ESI-FTICR MS

Mass spectra for accurate mass measurements were obtained on an Apex II FT-ICR mass spectrometer (Bruker Daltonics, Billerica, MA) equipped with a 7-T actively shielded superconducting magnet. Ions were introduced into the ion source via direct injection at a rate of 2 μl/min. Ions were generated with an Apollo pneumatically assisted electrospray ionization source (Bruker Daltonics, Billerica, MA) operating in the negative ion mode, and were accumulated in an rf-only external hexapole for 0.5–2 s before being transferred to the ion cyclotron resonance cell for mass analysis.

Mass spectra consist of 512k data points and are an average of 24–32 scans. The spectra were acquired using XMASS version 7.0.8 (Bruker Daltonics, Billerica, MA). For accurate mass measurements, spectra were internally calibrated with at least four known compounds bracketing the region of the ions of interest. DataAnalysis 3.4 (Bruker Daltonics, Billerica, MA) was used to determine elemental compositions.

3. Results and discussion

3.1. Identification and exact mass measurement of MSH

Mycothiol (Fig. 1) was previously observed in mass spectra of total lipid extracts from both *M. smegmatis* and *M. tuberculosis*, where it was used as a reduced-sulfur control in a screen for sulfated metabolites produced by mycobacteria [25]. Tandem MS, exact mass measurements, and isotopic labeling experiments were utilized to verify the identity of MSH in these extracts [25]. To further confirm these observations for this study, we analyzed crude

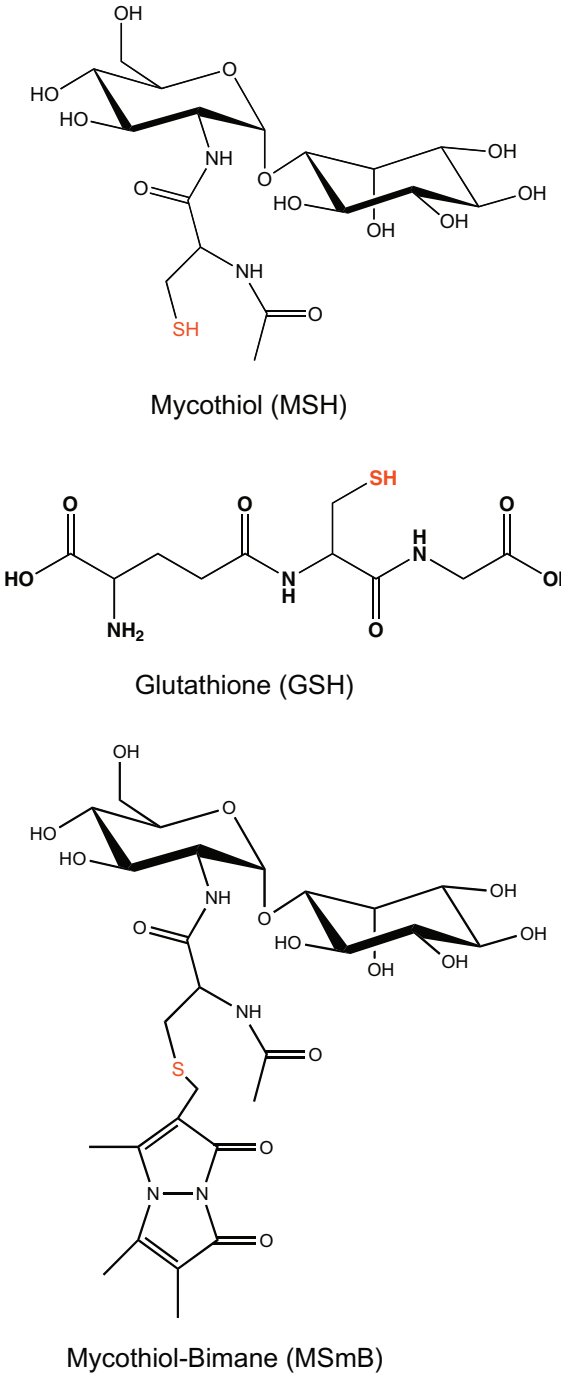

Fig. 1. The detailed chemical structures of mycothiol (MSH) and glutathione (GSH), and the bimane adduct of MSH (MSmB).

lipid extracts from *M. smegmatis* via high-resolution, high-mass-accuracy FT-ICR MS operating in the negative ion mode. Accurate mass measurements were used to measure the deprotonated MSH ion at *m*/*z* 485.1448, within 0.2 ppm of the theoretical mass (*m*/*z* 485.1447). Furthermore, a chloride adduct of MSH was measured at *m*/*z* 521.1211, within 0.4 ppm of the theoretical mass (*m*/*z* 521.1213) of the ion. Tandem MS experiments (data not shown) further establish the identity of these two ions.

In order to remove chloride as a possible counterion for MSH ionization, *M. smegmatis* crude carbohydrates were extracted with methanol to isolate the carbohydrates and to inactivate the cells. These extracts were resuspended in 1:1 acetonitrile:water for MS analysis. The resulting samples were free of the ion at *m*/*z* 521.12,

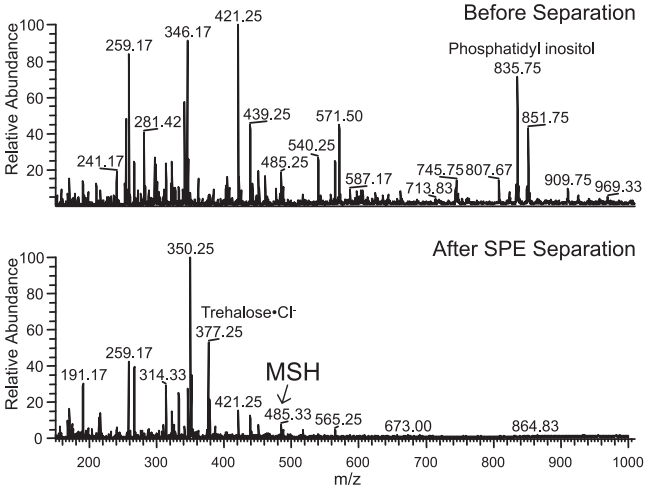

Fig. 2. Mass spectra of crude *M. smegmatis* carbohydrates before (top) and after (bottom) SPE separation.

leaving the ion at *m*/*z* 485.14 as the sole MSH species in these extracts.

3.2. SPE cleanup of MSH

The crude carbohydrate extracts obtained from *M. smegmatis* cells contained a number of lipid components such as multiple phosphatidylinositol lipoforms and other cell membrane lipids (Fig. 2, top), which could potentially complicate the relative quantification of MSH. In order to remove these non-carbohydrate components, the extracts were acidified and passed over an Oasis™ HLB cartridge. Ion-trap MS analysis revealed that MSH (*m*/*z* 485.25) and other *M. smegmatis* small carbohydrates eluted in the flowthrough (Fig. 2, bottom), while the lipid components eluted with methanol. The other small carbohydrates that eluted in the flow-through along with MSH are a chloride counterion adduct of trehalose at *m*/*z* 377.25, as well as other small disaccharides. Trehalose-2-sulfate, a significant component of the sulfated metabolome of *M. smegmatis* [26], is also present in this fraction as a deprotonated species at *m*/*z* 421.25. The intensity of MSH was somewhat improved after this purification step, although this improvement was not pronounced in all samples. Notably, the relatively abundant phosphatidylinositol (PI) lipids 18:1/16:0-PI (*m*/*z* 835.75) and 19:0/16:0 (*m*/*z* 851.75) present in the crude extract (Fig. 2, top) are absent from the carbohydrate fraction (Fig. 2, bottom).

3.3. Relative quantification of MSH

N,N-diacetylchitobiose (Fig. 3) was chosen as the internal standard (IS) for relative quantification because this compound is

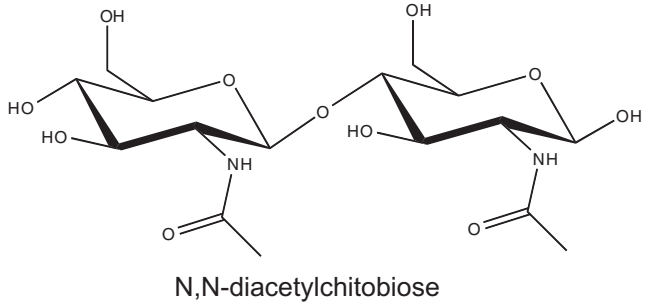

Fig. 3. The detailed chemical structure of N,N-diacetylchitobiose, the internal standard used in this study.

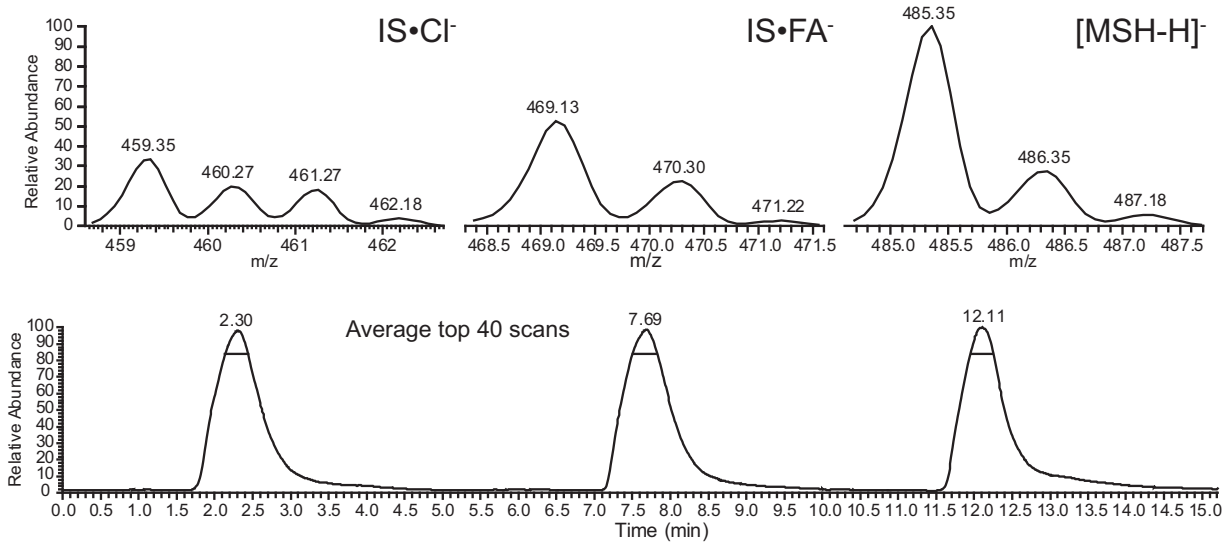

Fig. 4. TIC peak areas for MSH, IS·Cl⁻, and the IS·FA⁻ ions (top) were obtained by averaging the top 40 scans from each SIM spectra obtained via loop injection (bottom). Three injections were analyzed for each sample (bottom).

similar in structure and mass to that of MSH (Figs. 1 and 4). Ion trap MS analysis revealed that the IS is observed as both a chloride adduct at *m*/*z* 459, and a formate adduct at *m*/*z* 469 once spiked into *M. smegmatis* carbohydrate extracts (Fig. 4, top). Therefore, both forms of the IS as well as the deprotonated MSH species were analyzed via ion-trap MS using SIM and loop injection infusion. The top 40 scans from each injection were used to determine the total ion count peak areas for each ion, and the data were reported as the peak intensity ratio of the MSH ion to the sum of both IS ions (I_{MSH}/I_{IS}). Triplicate technical replicates obtained for each sample (Fig. 4, bottom) varied by no more than 8%, and were an average of 3.8% among each sample analyzed.

Triplicate biological samples for the WT and *mtr* samples were analyzed for relative MSH levels, while duplicate biological replicates for WT and *mtr* samples treated with H_2O_2 were analyzed (Table 1). The average relative MSH level for each type of sample is represented in Fig. 5. Interestingly, relative MSH levels between the replicate WT samples varied as much as two-fold, suggesting heterogeneity in MSH levels within biological replicates of a single type of sample.

When grown under standard conditions, no significant differences were observed in the average relative MSH levels between WT and mtr mutant samples (Fig. 5). These data are consistent with our observations that the *M. smegmatis mtr* mutant has no discernable growth phenotype *in vitro* (data not shown). Interestingly, peroxide treatment did not significantly affect the relative MSH levels in WT cells (Table 1, Fig. 5), however, upon treatment with hydrogen peroxide, the *mtr* samples show an average of about a 50% decrease in relative MSH levels (Fig. 5). The construction of an *mtr* mutant strain complemented with an intact *mtr* gene, along with the analysis of additional replicate samples, will be key to unraveling the role of Mtr in response to oxidative stress.

Table 1
Relative quantification of MSH levels for triplicate WT and *mtr* samples and duplicate WT and *mtr* samples treated with hydrogen peroxide, reported as the ratio of the peak intensities of the MSH ion to the IS ions (I_{MSH}/I_{IS}).

Sample	I_{MSH}/I_{IS}			Avg	StDev
	Rep 1	Rep 2	Rep 3		
WT	0.11	0.10	0.22	0.15	0.06
WT + H_2O_2	0.14	0.18	–	0.16	0.03
mtr	0.24	0.24	0.14	0.20	0.06
mtr + H_2O_2	0.13	0.10	–	0.12	0.02

3.4. Comparison to HPLC method

Lastly, we compared our method of relative quantification to the previously established protocol, which involves bromobimane labeling followed by HPLC analysis [23,24]. As seen in Fig. 6, the amount of MSH in the *mtr* sample was almost identical to that found in the parent strain (*i.e.*, 81% ± 15%). The components eluting at 12.5 min were measured at *m*/*z* 675.20 in the negative ion mode, consistent with the deprotonated form of the adduct of MSH, MSmB (Fig. 1). Control samples extracted in *N*-ethylmaleimide showed the expected loss of labeling (Fig. 6, bottom). These results are consistent with the data obtained from our MS-based method (Fig. 5), indicating that our method is a valid alternative to established methods of MSH quantification.

Our MS-based method offers a number of distinct advantages over the established HPLC method. Notably, our method provides inherent and rapid confirmation of the identity of MSH, while the previously established protocol requires additional MS confirmation to identify the MSmB derivative. Our method also shows higher reproducibility between technical replicates; triplicate technical replicates analyzed by our MS method varied by no more than

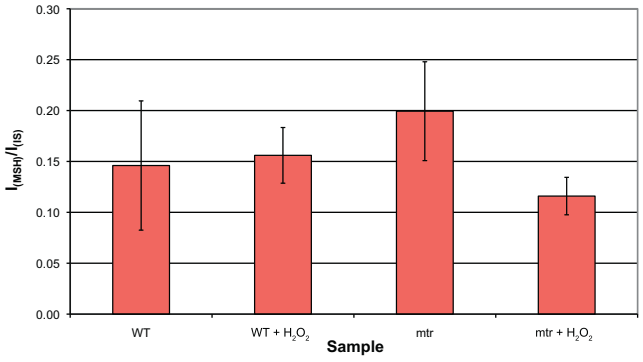

Fig. 5. The average relative levels of MSH for WT and *mtr* samples, with and without H_2O_2 treatment.

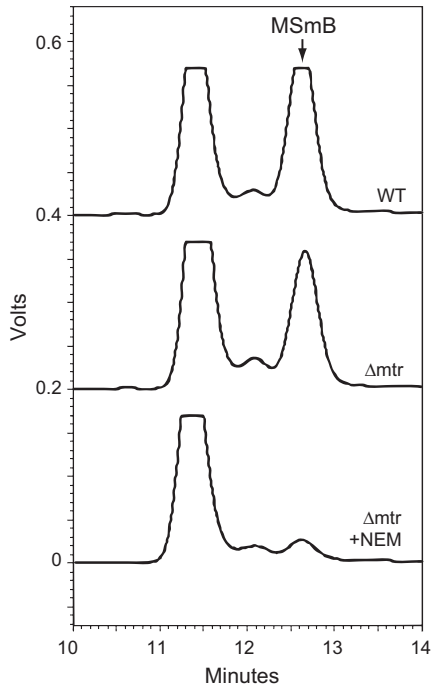

Fig. 6. MSH levels in WT and *mtr* samples derivatized with monobromobimane and analyzed by HPLC. The experiment was repeated in triplicate, and data from a single representative experiment are shown.

Table 2
Raw HPLC fluorescent intensity data for derivatized MSH from WT and *mtr* samples, with and without hydrogen peroxide treatment. Notably, these data lack normalization to an internal standard.

Sample	Raw intensity		Avg	StDev
	Rep 1	Rep 2		
WT	4.5e6	4.8e6	4.6e6	1.7e5
WT + H_2O_2	2.7e6	3.9e6	3.3e6	8.4e5
mtr	4.1e6	4.9e6	4.5e6	6.0e5
mtr + H_2O_2	1.6e6	3.0e6	2.3e6	9.9e5

8%. However, the variability between triplicate technical replicates analyzed by HPLC was over 25%. Table 2 shows the average raw intensity levels of the MSmB adduct for each type of sample, which, like our MS-based method, also show heterogeneity in MSH levels within biological replicates. Finally, it is of note that, like the MS data presented in Table 1, the HPLC data presented in Table 2 were obtained from equal amounts of cells for each sample. However, the data presented in Table 2 are not normalized to the intensity of an internal standard, which demonstrates an inherent weakness in the HPLC method.

4. Conclusions

In conclusion, we have developed a novel, rapid method to determine the relative quantification of MSH isolated from *M. smegmatis* extracts utilizing MS as the sole analytical technique. This method requires the utilization of common organic solvents with a low amount of hazardous waste materials, and very little purification is necessary. Only a brief, simple separation step to enrich the carbohydrate components is required for this method, and additional chromatographic instrumentation is not necessary. In contrast to the previously established methods of MSH quantification, this method does not require the use of light-sensitive reagents. We have applied this method to the analysis of WT and *mtr* samples to determine the relative levels of MSH in this mutant, with and without peroxide treatment. This method has potential applications to the quantification of MSH from other mycobacteria, including the pathogenic members of the *M. tuberculosis* complex.

Acknowledgments

J.A.L. acknowledges NIH #AI51622 for financial support of this research. K.S.C. acknowledges NIH #GM087638 for financial support of this research. The authors would like to thank members of the Leary lab for critical evaluation of this manuscript.

References

[1] Tuberculosis Fact Sheet No. 104, World Health Organization, 2007.
[2] J. Flynn, J. Chan, Tuberculosis: latency and reactivation, Infect. Immun. 69 (2001) 4195–4201.
[3] E. Houben, L. Nguyen, J. Pieters, Interaction of pathogenic mycobacteria with the host immune system, Curr. Opin. Microbiol. 9 (2006) 76–85.
[4] V. Deretic, S. Singh, S. Master, J. Harris, E. Roberts, G. Kyei, A. Davis, S. de Haro, J. Naylor, H.H. Lee, I. Vergne, Mycobacterium tuberculosis inhibition of phagolysosome biogenesis and autophagy as a host defence mechanism, Cell. Microbiol. 8 (2006) 719–727.
[5] J. Chan, J. Flynn, The immunological aspects of latency in tuberculosis, Clin. Immunol. (Orlando, FL) 110 (2004) 2–12.
[6] J.L. Flynn, J. Chan, Tuberculosis: latency and reactivation, Infect. Immun. 69 (2001) 4195–4201.
[7] T. Ulrichs, S.H. Kaufmann, New insights into the function of granulomas in human tuberculosis, J. Pathol. 208 (2006) 261–269.
[8] T. Jaeger, H. Budde, L. Flohé, U. Menge, M. Singh, M. Trujillo, R. Radi, Multiple thioredoxin-mediated routes to detoxify hydroperoxides in Mycobacterium tuberculosis, Arch. Biochem. Biophys. 423 (2004) 182–191.
[9] T. Jaeger, L. Flohé, The thiol-based redox networks of pathogens: unexploited targets in the search for new drugs, Biofactors 27 (2006) 109–120.
[10] N.S. Dosanjh, M. Rawat, J.H. Chung, Y. Av-Gay, Thiol specific oxidative stress response in Mycobacteria, FEMS Microbiol. Lett. 249 (2005) 87–94.
[11] G.L. Newton, K. Arnold, M.S. Price, C. Sherrill, S.B. Delcardayre, Y. Aharonowitz, G. Cohen, J. Davies, R.C. Fahey, C. Davis, Distribution of thiols in microorganisms: mycothiol is a major thiol in most actinomycetes, J. Bacteriol. 178 (1996) 1990–1995.
[12] M. Rawat, C. Johnson, V. Cadiz, Y. Av-Gay, Comparative analysis of mutants in the mycothiol biosynthesis pathway in Mycobacterium smegmatis, Biochem. Biophys. Res. Commun. 363 (2007) 71–76.
[13] G.L. Newton, P. Ta, K.P. Bzymek, R.C. Fahey, Biochemistry of the initial steps of mycothiol biosynthesis, J. Biol. Chem. 281 (2006) 33910–33920.
[14] N.A. Buchmeier, G.L. Newton, T. Koledin, R.C. Fahey, Association of mycothiol with protection of Mycobacterium tuberculosis from toxic oxidants and antibiotics, Mol. Microbiol. 47 (2003) 1723–1732.
[15] M. Rawat, Y. Av-Gay, Mycothiol-dependent proteins in actinomycetes, FEMS Microbiol. Rev. 31 (2007) 278–292.
[16] C. Vilchèze, Y. Av-Gay, R. Attarian, Z. Liu, M.H. Hazbón, R. Colangeli, B. Chen, W. Liu, D. Alland, J.C. Sacchettini, W.R. Jacobs, Mycothiol biosynthesis is essential for ethionamide susceptibility in Mycobacterium tuberculosis, Mol. Microbiol. 69 (2008) 1316–1329.
[17] G.L. Newton, R.C. Fahey, Mycothiol biochemistry, Arch. Microbiol. 178 (2002) 388–394.
[18] G.L. Newton, Y. Av-Gay, R.C. Fahey, A novel mycothiol-dependent detoxification pathway in mycobacteria involving mycothiol S-conjugate amidase, Biochemistry 39 (2000) 10739–10746.
[19] M.P. Patel, J.S. Blanchard, Expression, purification, and characterization of Mycobacterium tuberculosis mycothione reductase, Biochemistry 38 (1999) 11827–11833.
[20] C. Sassetti, D. Boyd, E. Rubin, Genes required for mycobacterial growth defined by high density mutagenesis, Mol. Microbiol. 48 (2003) 77–84.
[21] R.A. McAdam, S. Quan, D.A. Smith, S. Bardarov, J.C. Betts, F.C. Cook, E.U. Hooker, A.P. Lewis, P. Woollard, M.J. Everett, P.T. Lukey, G.J. Bancroft, W.R. Jacobs Jr., K. Duncan, Characterization of a Mycobacterium tuberculosis H37Rv transposon library reveals insertions in 351 ORFs and mutants with altered virulence, Microbiology (Reading, Engl.) 148 (2002) 2975–2986.
[22] D.P. Bhave, W.B. Muse, K.S. Carroll, Drug targets in mycobacterial sulfur metabolism, Infect. Disord. Drug Targets 7 (2007) 140–158.
[23] G.L. Newton, R.C. Fahey, Determination of biothiols by bromobimane labeling and high-performance liquid chromatography, Methods Enzymol. 251 (1995) 148–166.
[24] S.J. Anderberg, G.L. Newton, R.C. Fahey, Mycothiol biosynthesis and metabolism. Cellular levels of potential intermediates in the biosynthesis and degradation of mycothiol in mycobacterium smegmatis, J. Biol. Chem. 273 (1998) 30391–30397.

[25] J.D. Mougous, M.D. Leavell, R.H. Senaratne, C.D. Leigh, S.J. Williams, L.W. Riley, J.A. Leary, C.R. Bertozzi, Discovery of sulfated metabolites in mycobacteria with a genetic and mass spectrometric approach, Proc. Natl. Acad. Sci. U.S.A. 99 (2002) 17037–17042.

[26] J.D. Mougous, C.J. Petzold, R.H. Senaratne, D.H. Lee, D.L. Akey, F.L. Lin, S.E. Munchel, M.R. Pratt, L.W. Riley, J.A. Leary, J.M. Berger, C.R. Bertozzi, Identification, function and structure of the mycobacterial sulfotransferase that initiates sulfolipid-1 biosynthesis, Nat. Struct. Mol. Biol. 11 (2004) 721–729.